

Article

# Energy Management Strategy Design and Simulation Validation of Hybrid Electric Vehicle Driving in an Intelligent Fleet

Xin Ye <sup>1,2</sup>, Fei Lai <sup>1,2,\*</sup>  and Zhiwei Huo <sup>1,2</sup>

<sup>1</sup> Vehicle Engineering Institute, Chongqing University of Technology, Chongqing 400054, China; yexin@cqut.edu.cn (X.Y.); huozhiwei@163.com (Z.H.)

<sup>2</sup> Key Laboratory of Advanced Manufacturing Technology for Automobile Parts of Ministry of Education, Chongqing University of Technology, Chongqing 400054, China

\* Correspondence: laifeichq@cqut.edu.cn; Tel.: +86-1533-456-2987

Received: 17 October 2019; Accepted: 5 December 2019; Published: 10 December 2019



**Abstract:** This paper proposes a combination method of longitudinal control and fuel management for an intelligent Hybrid Electric Vehicle (HEV) fleet. This method can reduce the fuel consumption while maintaining the distance and speed for each vehicle in the fleet. An HEV system efficiency model was established to simulate the impact of different working modes. Based on the principle of optimal vehicle system efficiency, the energy management control strategy of HEV was designed. Then, the driver model of the piloting vehicle and the following vehicle was built by using an intelligent fuzzy control method. Finally, the intelligent fleet model and energy matching model of HEV were integrated with the simulation platform that was developed based on MATLAB/Simulink/Stateflow. The validity of the energy matching strategy of HEV under the principle of optimal system efficiency was verified by simulation results, and the purpose of improving the driving safety, traffic efficiency, and fuel economy of the fleet was achieved. Comparing with the conventional control strategy, the proposed method saved 7.79% of fuel for the HEV fleet. Meanwhile, the distance ranges between the vehicles were from 12 meters to 15 meters, which improved the driving safety, passing rate, and fuel economy.

**Keywords:** intelligent fleet; hybrid electric vehicle; system efficiency; energy management strategy; fuel economy

## 1. Introduction

As an important part of an advanced driving assistant system, vehicle autonomous queue driving can effectively control the speed based on the pre-set safety distance and improve the safety and passing rate during the driving [1–3]. However, it requires longitudinal control technology for a smart car. Meanwhile, the HEV is the best solution to achieve “energy saving and emission reduction” under the current technical level. To achieve this goal, the control strategy of energy matching for HEV is essential. The rapid development of future vehicles will drive the combination between hybrid and intelligent assisted driving technology, which will eventually lead to the achievement of low fuel consumption, low emission, safety, and intelligence.

For longitudinal control of intelligent vehicle, Tang et al. applied an artificial potential field to plan the expected motion state of vehicles [4–6]. Although the solution for conflict resolution was proposed, the factor of the passing rate was neglected. Lu et al. proposed a self-adaptive system for vehicle cruise control, and the dynamic model of a single lane vehicle was simulated under the hybrid traffic flow of smart cars [7–9]. Wang et al. quantified the impacts on the behaviors of vehicles

following in a string (or string stability) to establish potential performance enhancements of automated vehicle following systems from the aspects of the CACC algorithm, software system architecture, and module implementation [10–13]. The work mentioned in [10–13] improved the stability of traffic flow from the intelligent driving model and the collaborative adaptive cruise model. However, the energy optimization problem during the driving was ignored. Chu et al. proposed an energy efficient longitudinal driving strategy with a stop-and-go function to achieve full speed range driving [14–17]. The works in [14–17] optimized the energy saving under slow driving and intersection. For better results, more driving speed ranges should be analyzed. In general, the energy consumption of the car during longitudinal driving should be considered, especially in the energy optimization for the energy matching of HEV.

For passing rate and energy saving, Kitayama et al. used the radial basis function network (RBF) to optimize the variables in the torque control strategy of the internal combustion engine to improve the fuel economy for a parallel HEV [18,19]. Lin et al. proposed a framework of an adaptive control strategy for a series-parallel hybrid electric bus (SPHEB), based on the extracted hierarchical energy management strategy from dynamic programming (DP) and combined with driving pattern recognition (DPR) to improve the fuel economy [20]. Xu et al. proposed a double fuzzy control strategy combined with the braking energy recovery strategy, which took SoC, required torque, and bus speed as the inputs, and the double fuzzy control strategy obtained better fuel economy than the single fuzzy logic control strategy in the Chinese Bus Driving Cycle [21]. Jung et al. proposed a modified thermostatic control strategy for a parallel mild hybrid electric vehicle by operating internal combustion engine (ICE) in a high-efficiency region, and the vehicle's fuel economy was improved by 3.7% compared with that of the conventional strategy under urban driving [22]. Fu et al. proposed a parameter matching optimization method for hybrid electric vehicles based on multi-objective optimization (MOO), which used the weight coefficient method to transform the multi-objective optimization problem of fuel consumption and emissions into a single objective optimization problem to reduce significantly the fuel consumption and emissions of a vehicle simultaneously [23]. In [18–23], different energy management strategies were proposed for different hybrid vehicles, and the reduction of fuel consumption and emissions was verified by simulation analysis. The fusion algorithm of fleet control and energy saving control should also be considered. Li et al. demonstrated the fuel saving limitation and periodic fuel saving mechanism for both traditional and hybrid vehicles with respect to driving economy [24–26]. For a bus with an internal combustion engine and variable speed unit, the optimal fuel consumption was analyzed under impulse, sliding, and constant speed. The work in [26] proposed three optimal strategies for vehicle cruising, which were impulse speed and sliding, load state pulse and sliding, and constant speed cruise, respectively. However, the energy optimization matching of HEV during cruise was ignored. Zlocki et al. analyzed the improvement of potential fuel economy for hybrid vehicles from both theoretical calculation and experimental verification under ACC driving [27,28]. A methodology was proposed to quantify the fuel reduction potential for different driving strategies in ACC relevant driving scenarios. Sun et al. proposed a powertrain efficiency model of HEV based on situations of vehicle following, energy optimization of HEV, and economical HEV following, which showed that fusion control was theoretically superior to series control [29–31]. However, the energy consumption impact caused by energy loss of motor and battery efficiency was ignored. The SARTRE project in Europe, the ENERGY ITS project in Japan, and the GCDC project in the Netherlands have all shown that the vehicle queue stream could significantly reduce traffic congestion and improve traffic efficiency and fuel economy, which has become one of the leading directions for vertical control of smart vehicles [32–35]. At present, there is still a potential problem for the fuel consumption of the whole vehicle, which combines the efficiency of the hybrid vehicle engine and motor, the efficiency of battery charge and discharge, the efficiency of the transmission system, and the control of the transmission speed ratio.

In view of the current traffic congestion and the relative tail-end traffic accidents, the energy crisis, as well as environmental pollution, this paper proposes a control method of the combination of HEV

fleet control and energy saving. Based on the intelligent fuzzy control algorithm, the distance between vehicles was controlled, and the driving demands (speed and acceleration) of different vehicles were obtained. According to this requirement, the efficiency optimization model of the vehicle system under different working modes was established, and the efficiency optimization of the engine, motor, battery, and transmission system was carried out, while the energy matching control strategies of different vehicles in the driving process were obtained. Finally, the effectiveness of the control method was verified by simulation analysis. The paper’s organization is as follows: Section 1 gives the Introduction. In Section 2, the research object is chosen as a single axis parallel HEV with two clutches. The optimal efficiency model of HEV is established to ensure the energy optimization during driving in Section 3, which is based on the analysis of the operating mode characteristics of HEV. In Section 4, the intelligent fleet model and energy matching model of HEV are built with the simulation platform of MATLAB/Simulink/Stateflow. The validity of the energy matching strategy of HEV under the principle of optimal system efficiency is verified by simulation analysis, and the purpose of improving the driving safety, traffic efficiency, and fuel economy of the fleet is achieved. Conclusions are drawn in Section 5.

## 2. Research Object

This paper exploits a model HEV with a front-engine front-drive single axle parallel configuration. The parameters of the vehicle and the dynamic system are listed in Table 1. The structure of the single axle parallel HEV is shown in Figure 1.

**Table 1.** Parameters of the vehicle and dynamic system.

Parameters	Unit
Frontal area (A)	2.3 m <sup>2</sup>
Vehicle weight (m)	1548 kg
Vehicle weight with passengers (M)	1850 kg
Rolling resistance coefficient (f)	$f = f_0 + f_1(\frac{u_a}{100}) + f_4(\frac{u_a}{100})^4$
Wind resistance coefficient (CD)	0.34
Radius of wheel (r)	0.31 m
Main reduction ratio	4.625
Engine	1.6 L aluminum engine, 67 kW @ 6000 rpm, 160 Nm @ 4000–5000 rpm
Motor	25 kW
Battery	6.5 Ah, 288 V
Transmission ratio	5 AMT [3.461 1.869 1.235 0.948 0.809]

Note: HR grade tire was chosen (the maximum driving speed was 210 km/h). According to the drum experiments, the value ranges for rolling resistance coefficients  $f_0, f_1$ , and  $f_4$  were 0.0081–0.0098, 0.012–0.025, and 0.0002–0.0004, respectively.  $u_a$  is the driving speed.

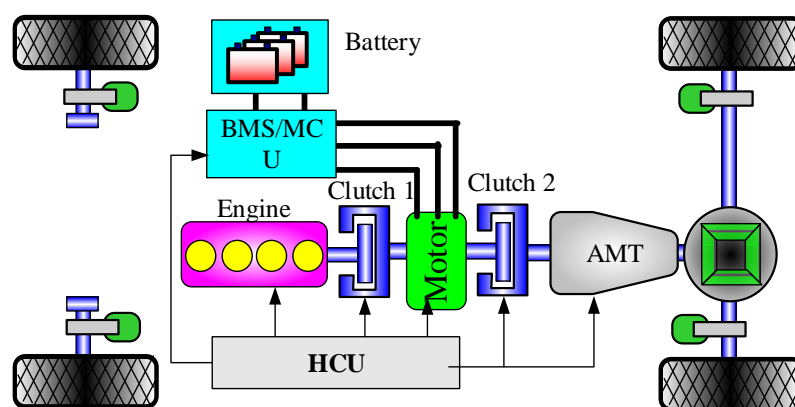


**Figure 1.** Single axle parallel HEV structure.

The value of the rolling resistance coefficient can be found in Table 2.

**Table 2.** The value of the rolling resistance coefficient under different driving speed.

$u_a$	20 km/h	40 km/h	60 km/h	80 km/h	100 km/h	120 km/h
$f$	0.0103	0.0108	0.0114	0.0120	0.0127	0.0136

### 3. Design of the Energy Control Strategy for HEV Based on Optimal System Efficiency

#### 3.1. Analysis of the Working Mode for HEV

The hybrid electric vehicle has different working modes due to its structural characteristics. The factors that affect the efficiency of the whole vehicle system are different under different working modes, which will affect the energy matching of the whole vehicle. Therefore, the efficiency characteristics of different working modes was analyzed first. Compared with the traditional vehicle, Clutch Number 1 of HEV can connect and disconnect the torque from the engine. The efficiency of the traditional vehicle will stay at a low level when the engine maintains the state of low speed and load or high speed and load, which lead to high fuel consumption and emission. However, the electric motor controlled by motor control unit (MCU) can solve this problem due to its characteristics. (1) Electric driving mode: the motor of HEV will drive the vehicle independently, which voids the low efficiency situation under the low speed and load of engine. (2) Light load charging mode: the engine will charge the battery to increase engine load rate. (3) Motor assistant mode: the motor will supply a part of the torque to reduce the load rate of the engine during high speed and load, which drive the engine to maintain optimal economy efficiency. (4) Engine drive mode: when the engine is under a high working ratio during the driving, the engine will drive the vehicle independently.

According to the above analysis, the driving modes of parallel HEV can be divided into electric driving mode, light load charging mode, motor assistant mode, and engine drive mode. By controlling the mode of the engine, motor, and clutch, the drive mode for HEV is switched. The various driving modes of HEV are listed in Table 3.

**Table 3.** Driving mode of HEV.

Driving Mode	Motor	Engine	Clutch Number 1
Electric driving mode	1	0	0
Light load charging mode	1	1	1
Motor assistant mode	1	1	1
Engine drive mode	0	1	1

Note: 1 means the motor or engine is working, or the clutch is connected. 0 means the motor or engine is off, or the clutch is disconnected.

#### 3.2. System Efficiency Model of Parallel HEV

In this subsection, the switching conditions for different driving modes of HEV are built according to the structure of the vehicle and the working mode of the motor, engine, and clutch. The switching condition of the driving mode was determined by the optimal efficiency of the vehicle system during the vehicle driving. According to the theory of vehicle dynamics, the dynamic equation of the transmission system for the vehicle can be established. The instant optimization of different driving modes is completed by the optimization of the efficiency of the vehicle driving system. The dynamic equation of a transmission system can be written as:

$$\begin{cases} \sum I_r \dot{\omega}_r + (I_m \dot{\omega}_m + I_e \dot{\omega}_e) i_g i_0 \eta_T = (T_e \pm T_m) i_g i_0 \eta_T - T_{req} \\ \omega_e = \omega_m = i_g i_0 \omega_r \end{cases} \quad (1)$$

where,  $I_r$ ,  $I_m$ , and  $I_e$  are the equivalent moment of inertia of the wheels and the moment of inertia of the motor and engine, respectively.  $\omega_r$ ,  $\omega_e$ , and  $\omega_m$  represent the angular velocity of the wheels, engine output shaft, and motor output shaft, respectively.  $T_{req}$  is the torque for the vehicle driving under a certain speed.  $T_e$  is the torque of the engine output shaft, and  $T_m$  is the torque of the motor output shaft.  $i_g$  and  $i_0$  stand for the transmission and final ratio, respectively.  $\eta_T$  is the efficiency of the transmission system. When  $T_e = 0$ , the vehicle is under electric driving mode,  $T_m = 0$ ; this means the engine drive mode, and the motor will be considered as an inertia flywheel. When  $T_m$  and  $T_e$  are both  $\neq 0$ ,  $T_m > 0$  and  $T_m < 0$  represent the motor assistant mode and light load charging mode, respectively.

In Equation (1), the relationship between the driving speed and rotation speed of tires can be written as:

$$\omega_r = u/r \tag{2}$$

where  $u$  stands for the driving speed and  $r$  is the radius of the tire. By derivation, Equation (2) will be re-written as:

$$\dot{\omega}_r = \frac{1}{r} du/dt \tag{3}$$

Based on Equation (3),  $\omega_e$  and  $\omega_m$  can be determined by:

$$\dot{\omega}_e = \dot{\omega}_m = \frac{1}{r} i_g i_0 du/dt \tag{4}$$

Rolling resistance, air resistance, acceleration resistance, and gradient resistance need to be calculated during the vehicle driving, which can be determined by:

$$F_{req} = mgf \cos \alpha + \frac{C_D A u^2}{21.15} + mg \sin \alpha + m \frac{du}{dt} \tag{5}$$

where  $m$  is the vehicle weight with passengers.  $f$  is the rolling resistance coefficient.  $C_D$  represents the wind resistance coefficient.  $A$  stands for the frontal area.  $u$  and  $\alpha$  are vehicle speed and the slope of the road, respectively. By the combination of all the above equations, the new definition of the system efficiency can be calculated by:

$$\frac{\sum I_r}{r} \frac{du}{dt} + (I_m + I_e) \frac{i_g^2 i_0^2}{r} \frac{du}{dt} \eta_T = (T_e \pm T_m) i_g i_0 \eta_T - (mgf \cos \alpha + mg \sin \alpha + \frac{C_D A}{21.15} u^2 + m \frac{du}{dt}) r \tag{6}$$

With Equation (6), different equations of system efficiency under various driving modes can be obtained.

### 3.2.1. Electric Driving Mode

The engine of parallel HEV is in a low load operating state with high fuel consumption and high emissions when driving at low speed and low loads. In this situation, if the SoC (state of charge) value of the battery is high, the clutch will disconnect, and the engine will stop. Meanwhile, the motor will drive the vehicle separately, and the power for driving the vehicle will be provided separately. By considering the transferring efficiency between battery and motor, with Equation (6), the system efficiency equation of this driving mode is determined as:

$$\left\{ \begin{aligned} \eta_{sys} &= \frac{P_{out}}{P_{in}} = \frac{P_{out}}{P_{bat}} = \left( \frac{mgfu \cos \alpha + \frac{C_D A u^3}{21.15} + mgu \sin \alpha + \delta m u \frac{du}{dt}}{T_m \omega_m} \right) \eta_m \eta_{dis-charge} \\ \delta &= 1 + \frac{\sum I_r}{mr^2} + \frac{I_m i_g^2 i_0^2 \eta_T}{mr^2} \end{aligned} \right. \tag{7}$$

In Equation (7),  $\eta_{sys}$  is the system efficiency for the whole vehicle,  $P_{bat}$  represents the power of the battery pack,  $P_{in}$  is the system input power under the electric driving mode, which is also the output

power of the battery,  $\eta_m$  is the motor efficiency,  $\eta_{dis-charge}$  is the battery discharge efficiency, and  $\delta$  is the conversion coefficient of the rotating mass.

### 3.2.2. Engine Only Mode

When the SoC value of the battery and the required power for the vehicle driving are both high, the engine will drive the vehicle separately. The engine maintains a middle or high load working state under high speed driving. By considering the transferring efficiency of the engine, with Equation (6), the system efficiency equation under this mode should be:

$$\begin{cases} \eta_{sys} = \frac{P_{out}}{P_{in}} = \left( \frac{mgfu \cos \alpha + \frac{C_D A u^2}{21.15} + mg \sin \alpha + \delta mu \frac{du}{dt}}{T_e \omega_e} \right) \eta_e \\ \delta = 1 + \frac{\sum I_r}{mr^2} + \frac{(I_m + I_e) i_g^2 i_0^2 \eta_T}{mr^2} \end{cases} \quad (8)$$

where  $P_{out}$  is the system output power under the engine drive mode,  $P_{in}$  stands for the system input power, which is also the output power of the engine, and  $\eta_e$  is the engine efficiency.

### 3.2.3. Hybrid Driving Mode

Light load charging mode and motor assistant mode are included. When the SoC value of the battery is insufficient and the required power of the vehicle driving is low, the engine will supply the power for the vehicle driving and charge the battery at the same time. At this time, the vehicle is in the light load charging mode. In this mode, the charge power for the battery is the system output, and the system efficiency equation for the vehicle is written as:

$$\begin{cases} \eta_{sys} = \frac{P_{out}}{P_{in}} = \left( \frac{mgfu \cos \alpha + \frac{C_D A u^2}{21.15} + mg \sin \alpha + \delta mu \frac{du}{dt} + P_{bat} \eta_{charge}}{T_e \omega_e} \right) \eta_e \\ \delta = 1 + \frac{\sum I_r}{mr^2} + \frac{(I_m + I_e) i_g^2 i_0^2 \eta_T}{mr^2} \end{cases} \quad (9)$$

where  $\eta_{charge}$  is the charging efficiency for the battery.

When the SoC value of the battery is sufficient and the required power for vehicle driving is out of the optimal engine working state, the torque generated by the engine and motor will be coupled to drive the vehicle, which is the motor assistant mode. In this mode, the power generated by the battery is the input of the system, which is a negative output. The system efficiency equation for the vehicle can be represented by:

$$\begin{cases} \eta_{sys} = \frac{P_{out}}{P_{in}} = \left( \frac{mgfu \cos \alpha + \frac{C_D A u^2}{21.15} + mg \sin \alpha + \delta mu \frac{du}{dt} - P_{bat} \eta_{dis-charge}}{T_e \omega_e} \right) \eta_e \\ \delta = 1 + \frac{\sum I_r}{mr^2} + \frac{(I_m + I_e) i_g^2 i_0^2 \eta_T}{mr^2} \end{cases} \quad (10)$$

In this driving mode, the motor is under the charging state in the former sub-mode and the motor is under the discharging mode in the latter one. Through model analysis, with the constraint of maximum efficiency for the vehicle system, the optimal solution for the motor working state can be determined under the given cycle conditions. The above model was analyzed under the constraints of the maximum output power, speed, torque of the engine, motor, and battery, as well as the maximum range of the SoC value and AMT speed ratio.

### 3.3. The Switching Pattern for the HEV under Various Driving Modes

According to efficiency optimization method determined by Section 3.2.2, based on the MATLAB simulation platform, the model of vehicle system efficiency was established in different driving modes, and the simulation results are shown in Figures 2 and 3. It can be seen that the electric driving mode

was much more efficient than the engine involved in driving, but the operating range is limited in Figure 2. Comparing the two surfaces in Figure 3, when the car was under the low speed load and high speed load driving, the vehicle system efficiency was low with the engine driving. By actively increasing the engine load (light charge) in the low speed load mode or by reducing the engine load (motor power) at high speed and load, the efficiency of the vehicle system was significantly improved.

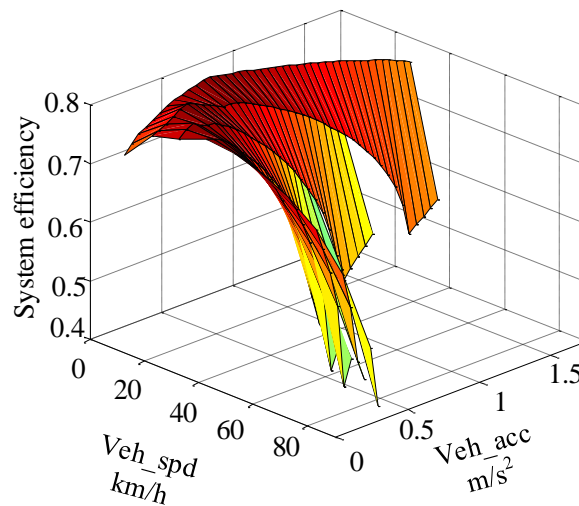


Figure 2. System efficiency in the electric driving mode.

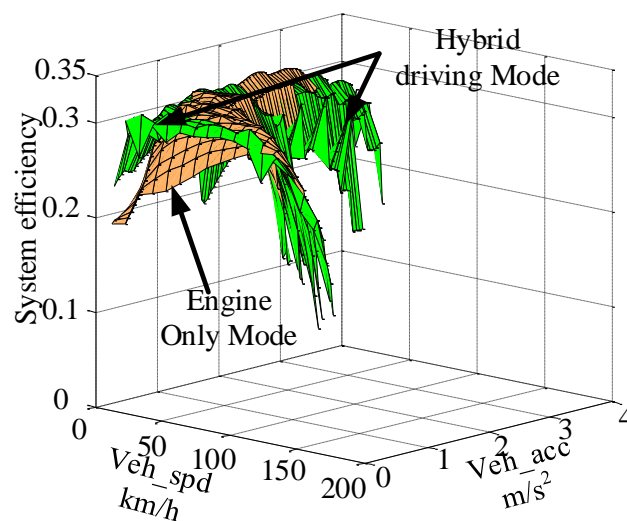


Figure 3. System efficiency of hybrid driving and the engine only mode.

The efficiency surface in Figure 3 was projected onto the “speed-acceleration” plane, and the working area for high efficiency of power source was obtained by considering the SoC of battery in Figure 4. A, B, C (C1, C2), and D are the light load charging mode, motor assistant mode, engine only mode, and electric driving mode, respectively. Line 1, Line 2, and Line 3 represent the switching boundaries of the light load charging mode and engine only mode, motor assistant mode and engine only mode, and engine only mode and electric driving mode, respectively. From the analysis in Section 3.2.2, the system efficiency of the vehicle showed the best performance under electric driving mode, which would improve the fuel economy. Line 3 is the boundary for the motor with full playing power under vehicle driving.

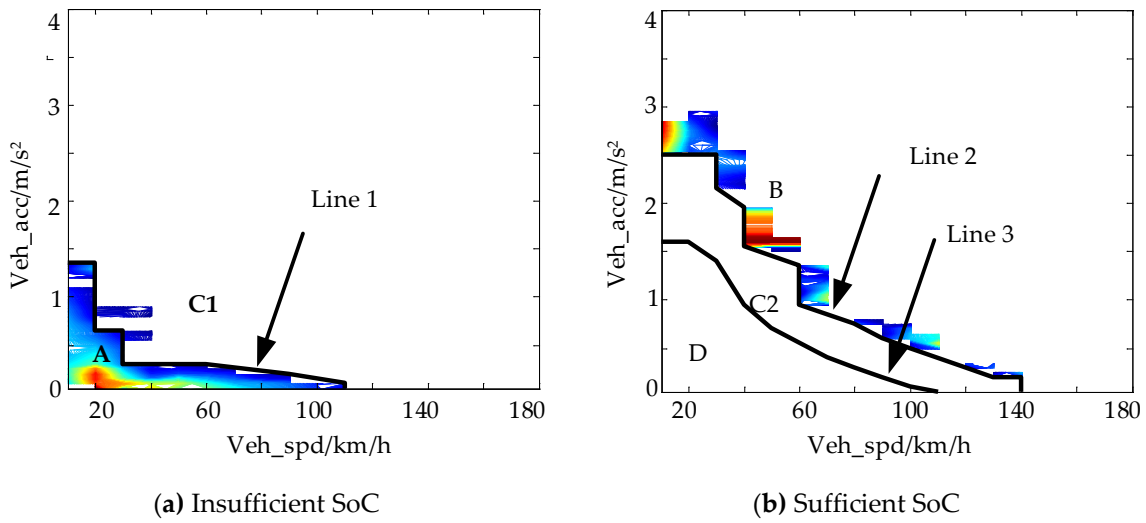


Figure 4. The shifting rules of HEV in the driving modes.

The three boundaries represent the working range of the engine and motor under different driving conditions (different vehicle speed, different acceleration). The power control method for HEV can be determined with these boundaries, which can also be called the energy management strategy.

#### 4. Modeling and Simulation Analysis with MATLAB/Simulink/Stateflow

##### 4.1. Modeling of the Smart Fleet for HEV

Three parallel HEVs were chosen for the smart fleet. The pilot vehicle of the fleet can self-drive according to the given drive cycle, and the following vehicles need to maintain a reasonable distance from the former vehicle, which will ensure the passing rate and driving safety. The model of the smart fleet is shown in Figure 5.

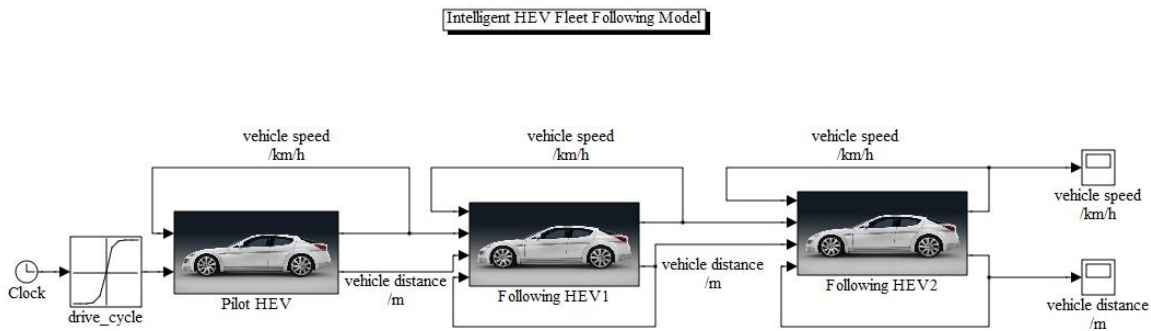


Figure 5. Intelligent HEV following model.

In Figure 5, Pilot HEV, Following HEV1, and Following HEV2 represent the pilot vehicle, Following Vehicle No. 1, and Following Vehicle No. 2, respectively. Based on the fuzzy control method, the mathematical model of the driver in the pilot vehicle was built by the difference between the speed of the pilot vehicle and the target vehicle speed  $\Delta u$  and the changing rate of the difference  $du/dt$ . Table 4 shows the relationships of the speed difference between the pilot and target vehicle and the changing ratio between gas and brake pedals.  $\Delta u$  and  $du/dt$  were divided into seven and six fuzzy subsets, respectively. NB, NM, NS, Z, PS, PM, and PB are negative big, negative middle, negative small, zero, positive small, positive middle, and positive big, respectively. P stands for the pedal. NB, NM, and NS stand for the brake pedal, and PS, PM, and PB represent the throttle pedal. The intelligent fuzzy control method was applied to determine the acceleration or brake degree of the pilot car, which is

shown in Table 4. The mathematical model of the driver based on MATLAB is shown Figure 6, which demonstrates the difference between the speed of pilot vehicle and target vehicle and the changing rate of the difference.  $K_d$  and  $K_b$  are control coefficients. The pilot vehicle dynamic model is the dynamic model of the pilot vehicle.

**Table 4.** Fuzzy rules of the driver. NB, NM, NS, Z, PS, PM, and PB are negative big, negative middle, negative small, zero, positive small, positive middle, and positive big, respectively. P stands for the pedal.

P $\Delta u$	$du/dt$							
	NB	NM	NS	Z	PS	PM	PB	
NB	PB	PB	PM	PS	PS	Z	NS	
NM	PM	PM	PS	PS	Z	Z	NS	
NS	PM	PS	PS	Z	Z	NS	NM	
PS	PS	PS	Z	Z	NS	NM	NB	
PM	PS	Z	Z	NS	NM	NB	NB	
PB	Z	Z	NS	NM	NB	NB	NB	

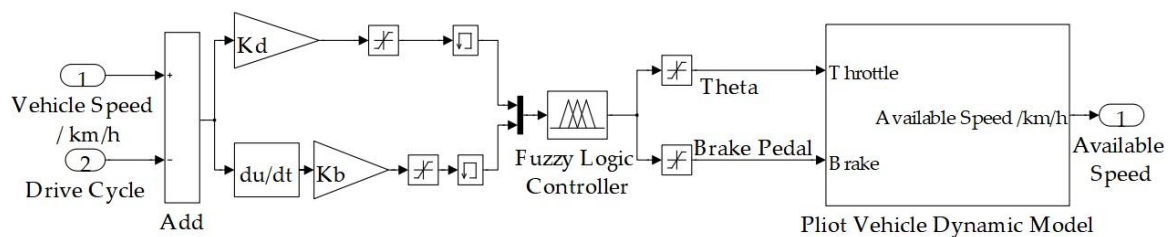


**Figure 6.** Driver model of the pilot vehicle.

The mathematical model of the driver for Following Vehicle No. 1 is shown in Figure 7. The opening degree of the accelerator or brake was determined by the differences of the speed and displacement between the pilot vehicle and Following Vehicle No. 1. Based on intelligent fuzzy control algorithms, the mathematical model for the following vehicle was built. The difference of speed  $\Delta u$  and the difference of displacement  $\Delta d$  were the inputs for the controller, and the degrees of the throttle and brake pedal were the outputs for the controller. The fuzzy control rules are listed in Table 5. The same control method was applied for Following Vehicle No. 2.

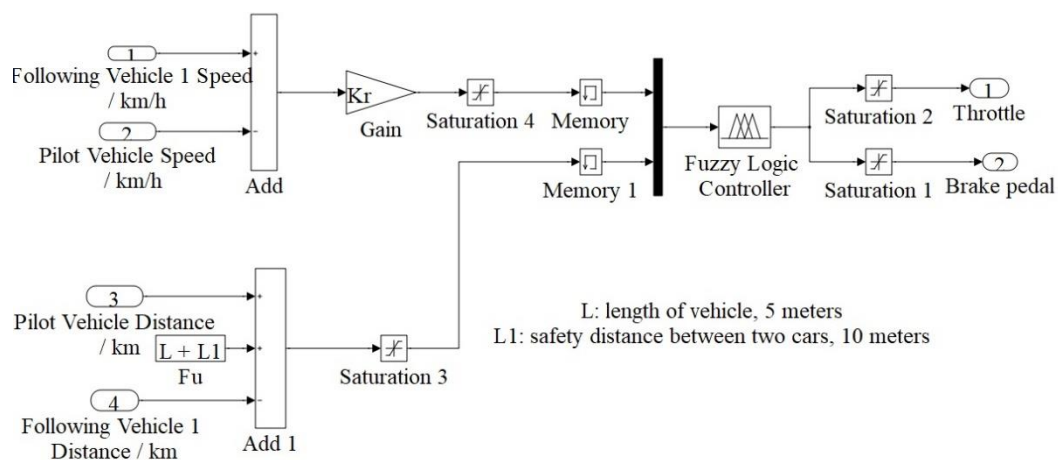


**Figure 7.** Driver model of following vehicle.

Table 5. Distance maintenance fuzzy rules.

P Δd	Δu							
	NB	NM	NS	Z	PS	PM	PB	
N	NS	NS	NS	NM	NM	NB	NB	
S	NS	NS	NS	NS	NM	NM	NB	
M	PB	PM	PS	Z	NS	NM	NB	
B	PB	PB	PB	PM	PM	PS	PS	

4.2. Modeling of the Energy Management Strategy for the Smart Fleet

In Section 3.1, by the satisfaction of the passing rate and safety, the required power for each vehicle in the fleet was determined under given drive cycle. In the next subsection, the energy matching strategy of HEV under various driving modes is established to ensure the system efficiency stayed at the optimal level under different conditions, which resulted in the improvement of the fuel economy for HEV. The recycling of braking energy was chosen from the parallel HEV braking energy case in the simulation software ADVISOR. In this section, a forward simulation model of HEV fleet is built, it includes models of the driver, gear shifting, energy matching, engine, motor, battery, and vehicle. The simulation model of the pilot vehicle is shown in Figure 8.

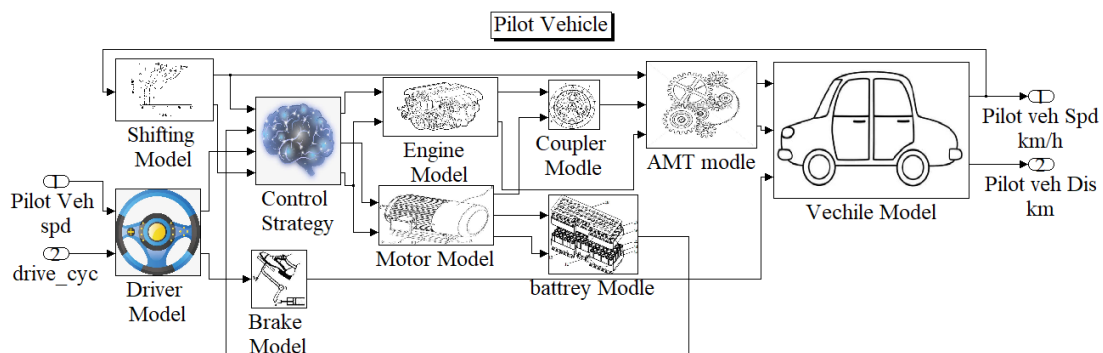
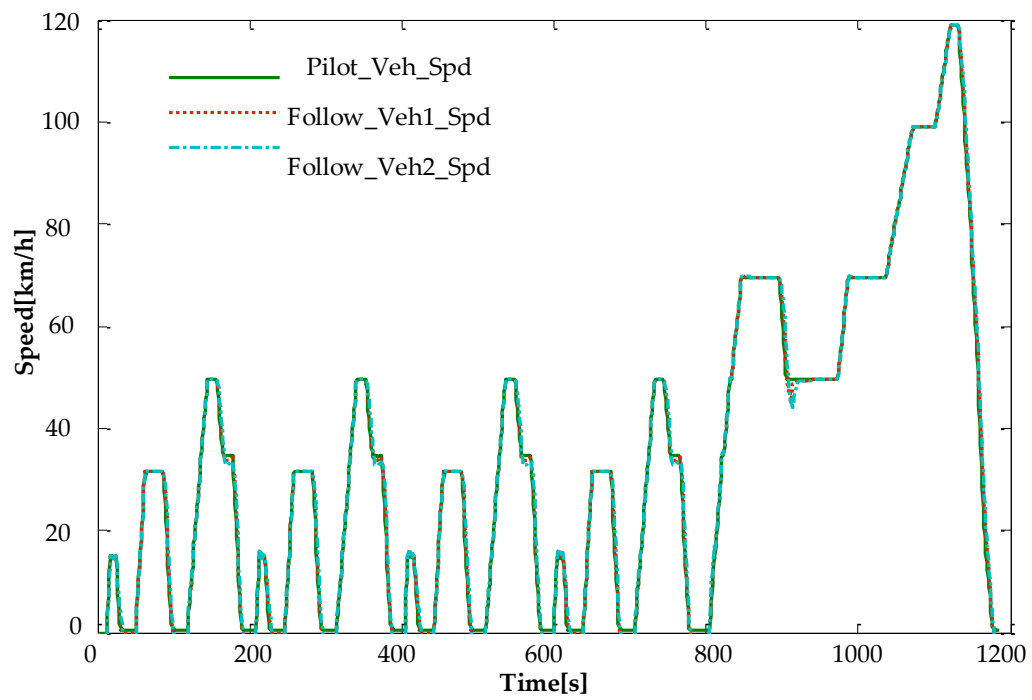


Figure 8. Forward model of the pilot HEV.

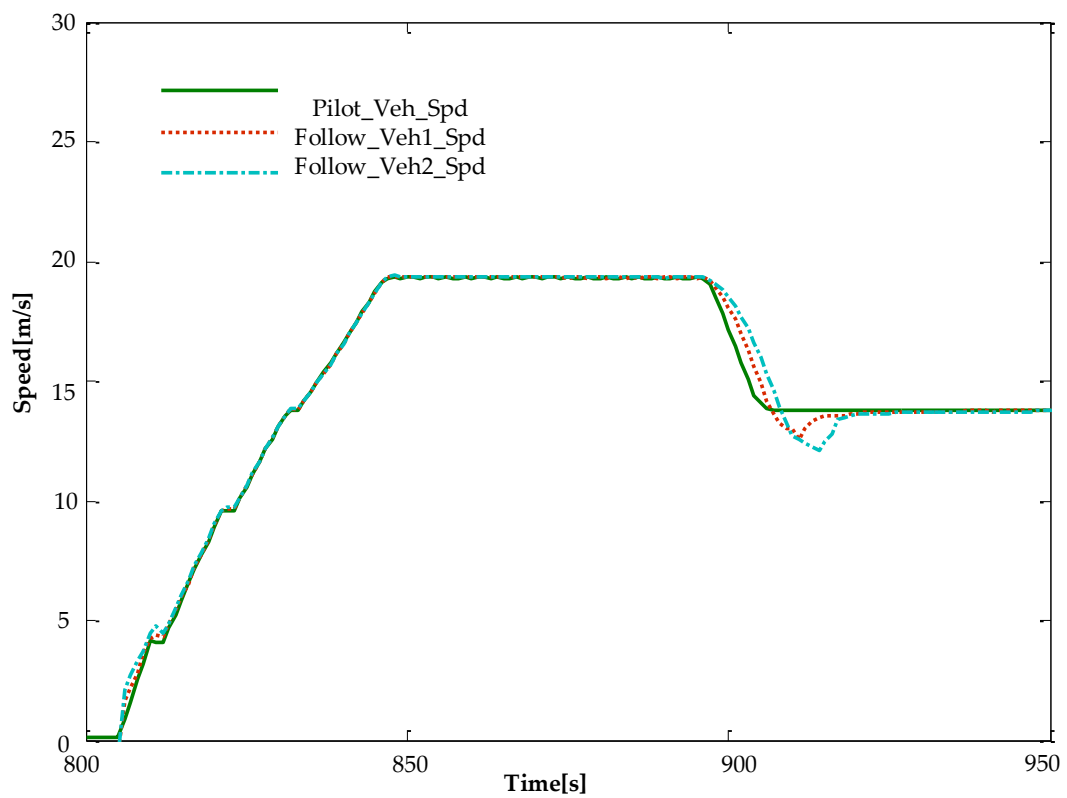
4.3. Verification of the Simulation

After building the model for the whole system, the simulation parameters were chosen. At the initial point  $t = 0$ , the headway between the vehicles was 15 m, and the lead vehicle started and followed the speed described by the NEDC drive cycle. The simulation time, traveling distance, and initial SoC were 1185 s, 10.9 km, and 0.7, respectively.

The relationships between the driving speed and distance of the vehicle and time are shown in Figures 9 and 10, respectively. The solid line is the changing trend for the pilot vehicle speed and distance. The dotted line is the changing trend of the speed and distance for Following Vehicle No. 1, and the dashed-dotted line is the changing trend of speed and distance for Following Vehicle No. 2. To observe the distance relationship between vehicles, Figure 10b shows the changing curve of the distance between the pilot vehicle and Following Vehicle No. 1 under the NEDC drive cycle.

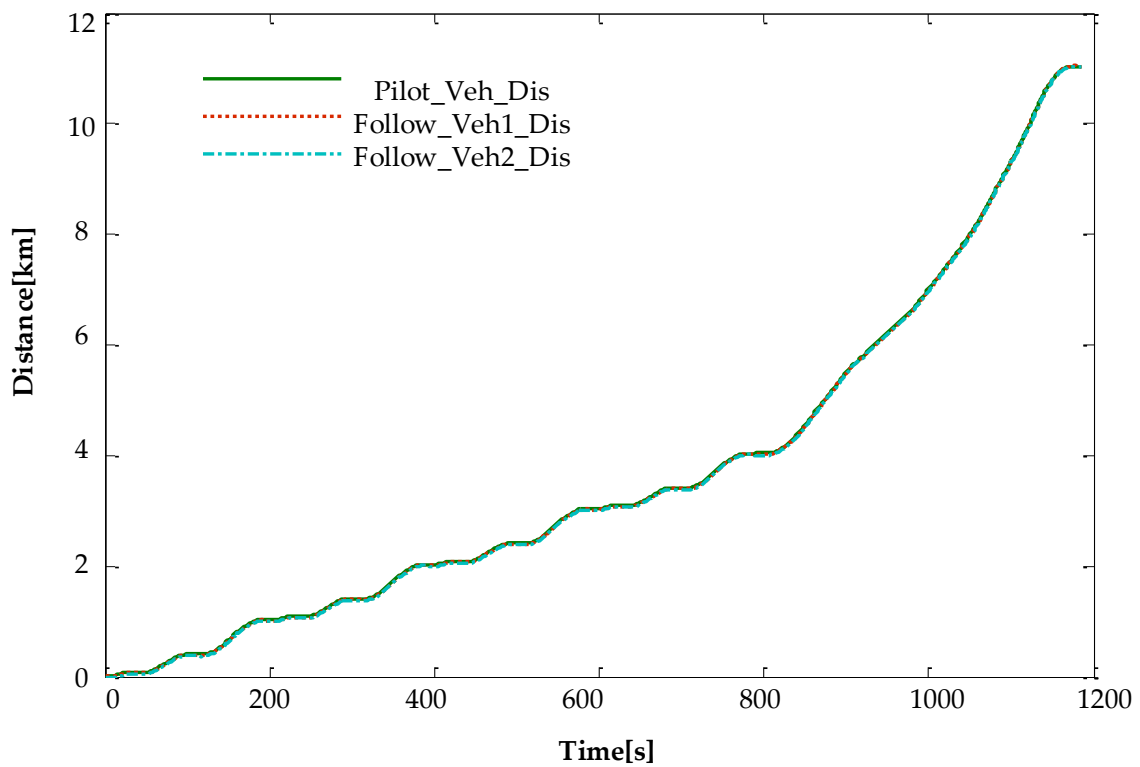


(a) Fleet vehicles' speed curve under NEDC.

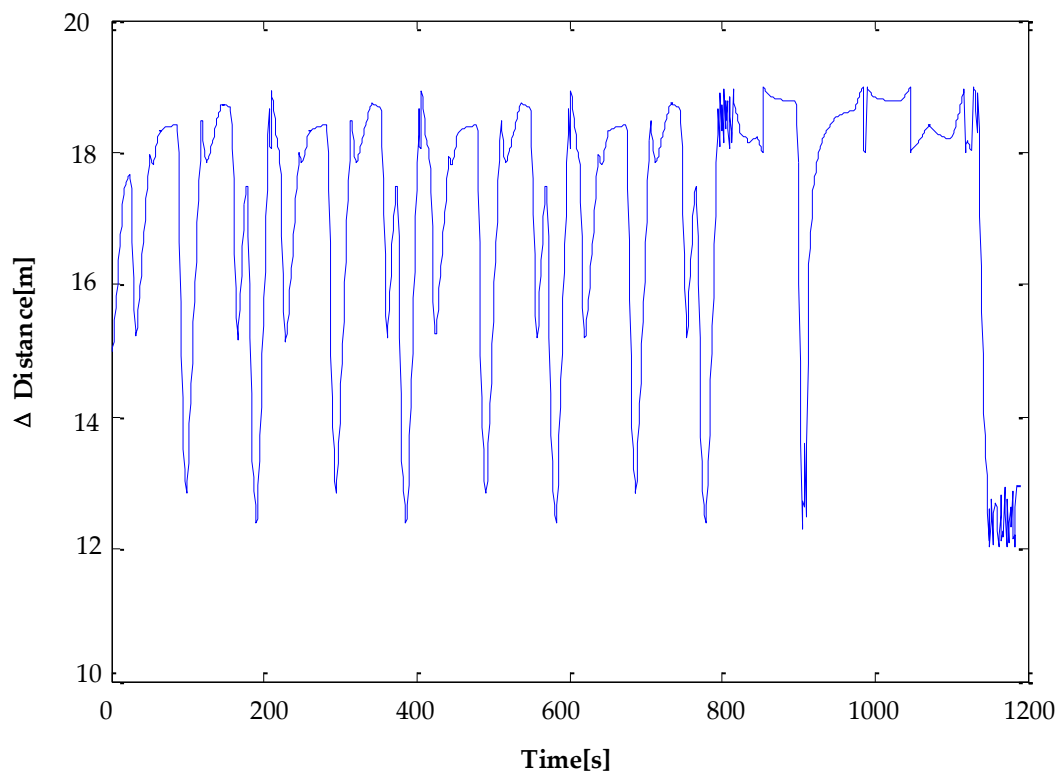


(b) Fleet vehicles' speed curve at 800–950 s.

Figure 9. Fleet vehicles' speed time.



(a) Driving distance change curve under NEDC.



(b) Head spacing change curve

Figure 10. Travel distance between fleet vehicles.

From Figure 9b, the largest speed difference between the vehicles existed in the time range of 910–920 s under the suburban condition. When  $t = 911$  s, the speed difference of the pilot vehicle

and Following Vehicle No. 1 was about 4 km/h. When  $t = 914$  s, the speed difference of Following Vehicle No. 1 and Following Vehicle No. 2 was about 5 km/h. As shown in Figure 10, the distances between each vehicle are relatively stable, the maximum and minimum distances being 19 m and 12 m, respectively. The maximum distance points occurred when the vehicle speed started to accelerate from 0 km/h or a constant speed and the changing rate of the accelerator pedal was large. The minimum distance point occurred at the end of braking, that is when the braking was completed, and the vehicle speed dropped to zero. Meanwhile, the changing rate of the brake pedal was relatively large. The large changing rate of acceleration and braking caused the oscillation of the distance between vehicles in the fleet. Compared with the initial vehicle distance, the ratio of positive disturbance was less than 28%, and the ratio of negative disturbance was less than 20%. The changing of resistance coefficients, delayed response, the function of vehicle distance, and other disturbance factors would cause this situation.

With the given NEDC drive cycle, the fuel economy of the traditional fleet and HEV fleet was compared. For the HEV fleet, this paper proposes a new energy management strategy to compare with the energy management strategy under the consideration of engine properties. The results are shown in Table 6.

**Table 6.** Fuel economy of intelligent HEV fleet.

	Internal Combustion Vehicle <sup>ⓐ</sup> *	Conventional Control Strategy <sup>ⓐ</sup> *	The New Control Strategy <sup>ⓐ</sup> *	$\Delta$ SoC	Compared with ③ and ①	Compared with ③ and ②
Pilot Vehicle	8.876	4.04	3.689	0.1296	↓58.43%	↓8.74%
Following Veh 1	7.581	4.15	3.818	0.1305	↓49.64%	↓8%
Following Veh 2	7.607	4.02	3.752	0.1314	↓50.68%	↓6.67%
Average	7.841	4.07	3.753	–	↓52.13%	↓7.79%

Note: The 100 km fuel consumption in \* is the comprehensive fuel consumption after converting the battery SoC.

## 5. Conclusions

Based on the driving safety and passing rate of the HEV fleet, this paper calculated the system efficiencies with different driving modes and established the energy management strategy with the optimal system efficiency. The longitudinal dynamic model of the HEV fleet was built under the restraints of vehicle distance and driving speed. In the last section, the longitudinal dynamic model and energy management strategic model were applied in the Matlab/Simulink/Stateflow simulation software. From the simulation results, under the given NEDC drive cycle, the maximum volatility was less than 28% and the maximum speed difference was less than 5 km/h, which met the road traffic efficiency and safety requirements. Since different vehicles in the fleet required different power, and the power supplements from engine and motor were various, which led to a difference of fuel consumption. Comparing to the traditional vehicle fleet, the HEV fleet with the proposed new energy management strategy saved 52.13% of fuel per 100 km, which saved 7.79% of fuel per 100 km compared to the energy management strategy under the consideration of the engine properties, on average.

The paper integrated the vertical control and energy matching technology of the HEV fleet, which achieved the improvement of the pass rate, driving safety, and fuel economy for HEV. However, the horizontal control problem for HEV was not considered, which is better for fleet control and energy saving technology under the actual driving case. Moreover, the standard NEDC is different from the actual road situation, and the analysis results would be more valuable with on-line prediction of the driving situation. Finally, the speed control and regenerative braking energy of the driving system should be optimized and analyzed at the same time, which would fully reflect the characteristics of the energy consumption in the operation of the HEV fleet.

**Author Contributions:** Conceptualization, X.Y. and F.L.; methodology, X.Y. and Z.H.; software, X.Y. and Z.H.; validation, X.Y. and F.L.; formal analysis, X.Y. and Z.H.; investigation, X.Y.; data curation, F.L.; writing—original draft preparation, X.Y.; writing—review and editing, X.Y.

**Funding:** This research was supported by the Science and Technology Research Program of Chongqing Municipal Education Commission (grant No. KJ1709231).

**Acknowledgments:** The authors would like to thank the anonymous reviewers for their valuable comments and suggestions. Special thanks to the simulation software of AVL Cruise and technical support provided by Key Laboratory of Advanced Manufacturing Technology for Automobile Parts of Ministry of Education, Chongqing University of Technology.

**Conflicts of Interest:** The authors declare no conflict of interest.

## Abbreviations

HEV	Hybrid Electric Vehicle
ACC	Adaptive Cruise Control
CACC	Cooperative Adaptive Cruise Control
GCDC	Grand Cooperative Driving Challenge
AMT	Automated Mechanical Transmission
BMS	Battery Management Strategy
HCU	Hybrid Control Unit
MCU	Motor Control Unit
SoC	State of Charge
NEDC	New European Driving Cycle
ADVISOR	ADvanced VehIcle SimulatOR

## References

- Li, J.; Cheng, H.; Guo, H.L. Survey on Artificial Intelligence for Vehicles. *Automot. Innov.* **2018**, *1*, 2–14. [[CrossRef](#)]
- Yang, D.G.; Jiang, K.; Zhao, D.; Yu, C.L.; Cao, Z.; Xie, S.C.; Xiao, Z.Y.; Jiao, X.Y.; Wang, S.J.; Zhang, K. Intelligent and connected vehicles: Current status and future perspectives. *Sci. China Technol. Sci.* **2018**, *61*, 1446–1471. [[CrossRef](#)]
- Milanes, V. Introduction to the Special Issue on Intelligent and Cooperative Vehicles. *Electronics* **2015**, *4*, 979–981. [[CrossRef](#)]
- Gu, X.P.; Han, M.X.; Zhang, W.S.; Xue, G.; Zhang, G.H.; Han, Y.P. Intelligent Vehicle Path Planning Based on Improved Artificial Potential Field Algorithm. In Proceedings of the 2019 International Conference on High Performance Big Data and Intelligent Systems (HPBD&IS), Shen Zhen, China, 9–11 May 2019; pp. 104–109.
- Liu, H.X.; Liu, F.; Zhang, X.J.; Guan, X.M.; Chen, J.; Savinaud, P. Aircraft conflict resolution method based on hybrid ant colony optimization and artificial potential field. *Sci. China Inf. Sci.* **2018**, *12*, 190–192. [[CrossRef](#)]
- Tang, R.Z.; Ji, J.; Wu, M.Y.; Fang, J.C.; Chen, M.Z. Vehicles Path Planning and Tracking Based on an Improved Artificial Potential Field Method. *J. Press Southwest Univ.* **2018**, *40*, 174–182. [[CrossRef](#)]
- Lu, C.R.; Aakre, A. A new adaptive cruise control strategy and its stabilization effect on traffic flow. *Eur. Transp. Res. Rev.* **2018**, *10*, 49. [[CrossRef](#)]
- Yu, S.W.; Shi, Z.K. The effects of vehicular gap changes with memory on traffic flow in cooperative adaptive cruise control strategy. *Phys. A Stat. Mech. Its Appl.* **2015**, *428*, 206–223. [[CrossRef](#)]
- Wang, J.M.; Rajamani, R. Adaptive Cruise Control System Design and Its Impact on Highway Traffic Flow. In Proceedings of the 2002 American Control Conference (IEEE Cat. No.CH37301), Anchorage, AK, USA, 8–10 May 2002; pp. 3690–3695. [[CrossRef](#)]
- Wang, P.W.; Wang, Y.P.; Yu, G.Z.; Tang, T.Q. An improved cooperative adaptive cruise control (CACC) algorithm considering invalid communication. *Chin. J. Mech. Eng.* **2014**, *27*, 468–474. [[CrossRef](#)]
- Sun, X.Q.; Zhang, H.Z.; Cai, Y.F.; Wang, S.H.; Chen, L. Hybrid modeling and predictive control of intelligent vehicle longitudinal velocity considering nonlinear tire dynamics. *Nonlinear Dyn.* **2019**, *97*, 1051–1066. [[CrossRef](#)]
- Meier, J.N.; Kailas, A.; Adla, R.; Bitar, G.; Moradi-Pari, E.; Abuchaar, O.; Ali, M.; Abubakr, M.; Deering, R.; Ibrahim, U.; et al. Implementation and evaluation of cooperative adaptive cruise control functionalities. *IET Intell. Transp. Syst.* **2018**, *12*, 1110–1115. [[CrossRef](#)]
- Woo, J.W.; Yu, S.B.; Lee, S.B. Design and simulation of a vehicle test bed based on intelligent transport systems. *Int. J. Automot. Technol.* **2016**, *17*, 353–359. [[CrossRef](#)]

14. Chu, H.Q.; Guo, L.L.; Yan, Y.J.; Gao, B.Z.; Chen, H.; Bian, N. Energy-efficient longitudinal driving strategy for intelligent vehicles on urban roads. *Sci. China* **2019**, *62*, 64201. [[CrossRef](#)]
15. Kamal, M.A.S.; Mukai, M.; Murata, J.; Kawabe, T. Model Predictive Control of Vehicles on Urban Roads for Improved Fuel Economy. *IEEE Trans. Control Syst. Technol.* **2013**, *21*, 831–841. [[CrossRef](#)]
16. HomChaudhuri, B.; Lin, R.; Pisu, P. Hierarchical control strategies for energy management of connected hybrid electric vehicles in urban roads. *Transp. Res. Part C Emerg. Technol.* **2016**, *62*, 70–86. [[CrossRef](#)]
17. Yu, K.; Tan, X.; Yang, H.; Liu, W.; Cui, L.; Liang, Q. Model Predictive Control of Hybrid Electric Vehicles for Improved Fuel Economy. *Asian J. Control* **2016**, *18*, 2122–2135. [[CrossRef](#)]
18. Kitayama, S.; Saikyo, M.; Nishio, Y.; Tsutsumi, K. Torque control strategy and optimization for fuel consumption and emission reduction in parallel hybrid electric vehicles. *Struct. Multidiscip. Optim.* **2015**, *52*, 595–611. [[CrossRef](#)]
19. Kitayama, S.; Saikyo, M.; Nishio, Y.; Tsutsumi, K. Torque control strategy incorporating charge torque and optimization for fuel consumption and emissions reduction in parallel hybrid electric vehicles. *Struct. Multidiscip. Optim.* **2016**, *54*, 177–191. [[CrossRef](#)]
20. Lin, X.Y.; Li, H.L. Adaptive Control Strategy Extracted from Dynamic Programming and Combined with Driving Pattern Recognition for SPHEB. *Int. J. Automot. Technol.* **2019**, *20*, 1009–1022. [[CrossRef](#)]
21. Xu, Q.W.; Luo, X.X.; Jiang, X.B.; Zhao, M. Research on Double Fuzzy Control Strategy for Parallel Hybrid Electric Bus. In Proceedings of the International Conference on Life System Modeling and Simulation, LSMS 2017 and International Conference on Intelligent Computing for Sustainable Energy and Environment, ICSEE 2017, Nanjing, China, 22–24 September 2017; pp. 362–370. [[CrossRef](#)]
22. Jung, D.B.; Cho, S.W.; Park, S.J.; Min, K.D. Application of a modified thermostatic control strategy to parallel mild HEV for improving fuel economy in urban driving conditions. *Int. J. Automot. Technol.* **2016**, *17*, 339–346. [[CrossRef](#)]
23. Fu, X.L.; Zhang, Q.; Tang, J.Y.; Wang, C. Parameter Matching Optimization of a Powertrain System of Hybrid Electric Vehicles Based on Multi-Objective Optimization. *Electronics* **2019**, *8*, 875. [[CrossRef](#)]
24. Li, S.; Peng, H. Strategies to Minimize the Fuel Consumption of Passenger Cars During Car-following Scenarios. *Proc. Inst. Mech. Eng. Part D J. Automob. Eng.* **2011**, *226*, 419–429. [[CrossRef](#)]
25. Li, S.B.; Xu, S.B.; Huang, X.Y.; Cheng, B.; Peng, H. Eco-departure of Connected Vehicle with V2X Communication at Signalized Intersections. *IEEE Trans. Veh. Technol.* **2015**, *64*, 5439–5449. [[CrossRef](#)]
26. Xu, S.; Li, S.; Peng, H.; Cheng, B.; Zhang, X.W. Fuel-saving Cruising Strategies for Parallel HEVs. *IEEE Trans. Veh. Technol.* **2016**, *65*, 4676–4686. [[CrossRef](#)]
27. Zlocki, A.; Themann, P. Methodology for quantification of fuel reduction potential for adaptive cruise control relevant driving strategies. *IET Intell. Transp. Syst.* **2014**, *8*, 68–75. [[CrossRef](#)]
28. Flehmig, F.; Kästner, F.; Knödler, K.; Knoop, M. Eco ACC for Electric and Hybrid Electric Vehicles. *ATZ Worldw.* **2014**, *1161*, 10–15. [[CrossRef](#)]
29. Sun, Y.; Wang, X.Y.; Li, L.; Shi, J.L.; An, Q. Modelling and control for economy-oriented car-following problem of hybrid electric vehicle. *IET Intell. Transp. Syst.* **2019**, *13*, 825–833. [[CrossRef](#)]
30. Tajeddin, S.; Vajedi, M.; Azad, N.L. A Newton/GMRES Approach to Predictive Ecological Adaptive Cruise Control of a Plug-in Hybrid Electric Vehicle in Car-following Scenarios. *IFAC-Pap.* **2016**, *49*, 59–65. [[CrossRef](#)]
31. Li, L.; Wang, X.Y.; Song, J. Fuel consumption optimization for smart hybrid electric vehicle during a car-following process. *Mech. Syst. Signal Process.* **2017**, *87*, 17–29. [[CrossRef](#)]
32. Kamal, M.A.S.; Mukai, M.; Kawabe, T.; Murata, J. Ecological Vehicle Control on Roads with Up-down Slopes. *IEEE Trans. Intell. Transp. Syst.* **2011**, *12*, 783–794. [[CrossRef](#)]
33. Xu, S.B.; Li, S.B.; Cheng, B.; Li, K.Q. Instantaneous Feedback Control for a Fuel-Prioritized Vehicle Cruising System on Highways with a Varying Slope. *IEEE Trans. Intell. Transp. Syst.* **2016**, *18*, 1210–1220. [[CrossRef](#)]
34. Luo, L.H.; Liu, H.; Li, P.; Wang, H. Model predictive control for adaptive cruise control with multi-objectives: Comfort, fuel-economy, safety and car-following. *J. Zhejiang Univ. Sci. A* **2010**, *11*, 191–201. [[CrossRef](#)]
35. Li, S.E.; Zheng, Y.; Li, K.Q.; Wang, J.Q. An Overview of Vehicular Platoon Control under the Four-Component Framework. In Proceedings of the 2015 IEEE Intelligent Vehicle Symposium, Seoul, Korea, 28 June–1 July 2015; pp. 286–291. [[CrossRef](#)]

